geoconvention
Virtual Event
September 21-23
2020
CSPG · CSEG · CWLS · GAC · MAC · IAH

3D Full waveform inversion for land dataset in the presence of topography variations

Amsalu Y. Anagaw and Mauricio D. Sacchi

Signal Analysis and Imaging Group (SAIG), Department of Physics, University of Alberta

Summary

Full waveform inversion (FWI) has the potential to produce accurate and high-resolution subsurface structures of the Earth model from observed field data. However, many problems exist associated with FWI that hinders its practical applications to large scale 3D geophysical inverse problems. In the presence of complex surface topography, one of the main problems challenging the successful application of 3D FWI to land dataset is due to the high nonlinearity properties introduced by free-surface effects as well as source and receiver representations in the grid and their signature estimations in the numerical forward modeling.

For land areas with irregular surface topography, the efficiency and accuracy of subsurface model reconstruction from FWI require the accuracy of numerical simulation of the seismic wavefield that takes into account for effects of surface topography. The standard finite-difference scheme computing seismic wave propagation in the earth implicitly assumes uniform structured grids and often provides diffraction artifacts generated by the staircase irregular boundary surface. To avoid numerical artifacts generates from the finite-difference approximation near the irregular topographic surface, we present the ghost extrapolation method for estimating the values of the wavefield at and near the irregular free surface. In addition to the ghost wavefield extrapolations, exact representations of source and receiver locations in the numerical grid improve the estimation of acoustic velocity model by FWI.

Introduction

The main objective of full waveform inversion (FWI) is to produce high-fidelity velocity model at various scales from near-surface to global or to improve the accuracy of the velocity model employed by the conventional seismic migration methods, such as reverse time migration, depth migration etc, to produce depth images with reflectors in correct lateral and depth positions, and also achieves better focus (Stekl and Pratt, 1998; Vigh et al., 2009; Virieux and Operto, 2009; Zhang et al., 2015).There are many reasons why FWI is preferable over conventional velocity model building, where the conventional methods fail. Complex near-surface velocity structure in shallow areas has the potential for large, rapid velocity variations due to many reasons, and conventional ray-based tomography methods will fail in particular if large near-surface velocity contrasts are present. 3D FWI on land seismic datasets is very challenging due to the effects of near-surface heterogeneities on seismic reflections (Lemaistre et al., 2018). For land areas with irregular surface topography, the efficiency and accuracy of subsurface model reconstruction from FWI require the accuracy of numerical simulation of the seismic wavefield that takes into account for effects of surface topography.

In numerical modeling of seismic wave propagation in the earth, one of the most common numerical schemes for solving the wave equation is based on the finite-difference (FD) approximation. However, the FD scheme implicitly assumes uniform structured grids and encounters a problem in treating the free and irregular topographic surface. For land FWI, accurate source and receiver location implementations are also essential. To avoid numerical artifacts generates from the FD approximation near the irregular topographic surface, we have improved the FD scheme by incorporating Lagrangian polynomial interpolation of wavefield values at and near the irregular free surface. Thus, diffraction artifacts generated by staircase finite-difference approximation from an arbitrarily irregular surface can

be eliminated. The improved FD approximate scheme outside the irregular topography boundaries takes into account ghost cell values, and a mirror flow extrapolation obtains their values.

In addition to incorporating the 3D interpolations of wavefield values at and near the topography surface in the finite-difference approximation, source and receiver locations at the arbitrary position are taking into account to their exact locations in FD schemes using Kaiser windowed $sinc$ functions (Hicks, 2002). The 3D FWI results show the combination of ghost wavefield extrapolation method near and at the irregular topographic surface, and exact representations of source and receiver locations in the FD scheme improves both the resolution and accuracy of the reconstructed velocity model by FWI. The use of ghost extrapolations near the irregular free surface in the numerical modeling eliminates artifacts generated by the staircase boundary. Hence, FWI achieves more accurate and reliable results. In this paper, we present a 3D acoustic simultaneous-source time-domain FWI results on the SEG/EAGE Overthrust velocity model to highlight our premises.

Theory

FWI aims to find the subsurface model by minimizing the least-squares misfit between the observed $\mathbf{d}^{obs}$ and modeled data $\mathbf{d}^{cal}(\mathbf{m})$

$$J(\mathbf{m}) = \frac{1}{2} \parallel \mathbf{d}^{obs} - \mathbf{d}^{cal}(\mathbf{m}) \parallel_2^2 . \tag{1}$$

The minimization of the misfit function is a nonlinear problem in which, from observed wavefields, one attempts to estimate the P-wave velocity model $\mathbf{m}$. For synthetic modeling $\mathbf{d}^{cal}(\mathbf{m})$, our work pertains to seismic wave propagation in a three-dimensional (3D) acoustic medium. The 3D acoustic wave propagation modeling is performed with a staggered-grid scheme using 2^{nd} order in time and 4^{th} order in space as

$$\begin{aligned}
\frac{\partial P}{\partial t} &= \kappa \left(\frac{\partial V_x}{\partial x} + \frac{\partial V_y}{\partial u} + \frac{\partial V_z}{\partial z} \right) \\
\frac{\partial V_x}{\partial t} &= \frac{1}{\rho_x} \frac{\partial P}{\partial x} + f_x \\
\frac{\partial V_y}{\partial t} &= \frac{1}{\rho_y} \frac{\partial P}{\partial y} + f_y \\
\frac{\partial V_z}{\partial t} &= \frac{1}{\rho_z} \frac{\partial P}{\partial y} + f_z
\end{aligned} \tag{2}$$

where $\kappa = \rho v^2$, ρ is the density of the medium, V_x,V_y and V_z are particle velocities in x, y and z direction respectively.The terms f_x, f_y and f_z represent the source signatures in x, y and z direction respectively.

For any arbitrary source and receiver position, sources and receivers can be located at their correct locations anywhere within the model in the finite-difference schemes using Kaiser windowed $Sinc$ Hicks (2002). A windowed $Sinc$ function approximates accurate implementation of point source and receiver at an arbitrary position in a coarse grid (Hicks, 2002)

$$sinc(x) = \frac{sin(\pi x)}{x} \tag{3}$$

where for a point source $x = (x_g - x_s)$, and for a receiver position $x = (x_g - x_r)$; x_g represents the position of the grid nodes, x_s represents the position of the source and x_r represents the positions

of the receiver. The finite impulse response filter of the point source and receiver, the $Sinc$ function is then tapered with a Kaiser window function to limit its spatial support (Hicks, 2002; Bergen and Antoniou, 2005)

$$W(x) = \begin{cases} \frac{I_o(b\sqrt{1-(x/r)^2})}{I_o(b)} & for - r \leq x \leq r \\ 0 & otherwise \end{cases} \tag{4}$$

where r is the window half-width, I_o is the zero-order modified Bessel function of the first kind, and b is the parameter that controls the shape of a Kaiser window.

The irregular free surface topography for wave propagation at and near the topography surface boundaries are into account explicitly into numerical computations by using ghost points above the free surface. The solutions to Eqn.2 at and near the surface boundary require using the 4^{th} order finite-difference approximation requires the ghost cell values of points beyond the free surface. For the 3D model, values at ghost points (mirror points) outside the modeling domain are obtained using accurate polynomial interpolation method along each direction: x, y and z

$$P(x)_j = y_j \prod_{k=0,k\neq j}^{n} \frac{x - x_k}{x_j - x_k}, \tag{5}$$

where $P(x)$ is the Lagrange interpolating polynomial of degree $\leq (n-1)$ that passes through the n points $(x_1, y_1 = P(x_1))$, $(x_2, y_2 = P(x_2))$ ... $(x_n, y_n = P(x_n))$.

The nonlinear 3D time-domain full waveform inversion aims to minimize the difference between the observed and the synthetic data obtained from an initial model $\mathbf{m_0}$ by iteratively updating the model in the direction of steepest descent of the misfit function $J(\mathbf{m})$ as follows:

$$\mathbf{m}_{k+1} = \mathbf{m}_k - \alpha_k \nabla_{\mathbf{m}} J(\mathbf{m}_k), \tag{6}$$

where α_k is step length of the k^{th} iteration (Nocedal and Wright, 2006).

Example

For 3D FWI, we use the SEG/EAGE Overthrust velocity model with topography, as shown in Figure 1a. Figure 1b is the smooth velocity model used as the starting model for the inversion. The SEG/EAGE Overthrust velocity model was gridded onto a coarser grid of size 50 m by 50 m. Synthetic data were generated in a time-domain acoustic wave equation via a finite-difference approximation. For inversion, we used a total number of 1089 sources and 9801 receivers that are arbitrarily placed. Sources and receivers are arbitrarily placed below the topography surface. To compute the data, we used a source signature modeled by a Ricker wavelet with a 10 Hz central frequency.

For inversion, to speed up the 3D FWI computation, we use a source encoding technique. The source encoding scheme contains 60 super-shots, and each super-shot includes 18 individual sources. To mitigating the non-linearity in the FWI, the inversion is performed in a multiscale stage from low to high frequencies data (Bunks et al., 1995). For inversion, we run the iterative process using multiscale approaches in the time domain with increasing frequency bandwidth (0.0-6.5Hz, 0.0-8.5Hz, 0.0-11.0Hz, 0.0-15.5Hz, 0.0-19.5Hz, 0.0-22.5Hz). For each frequency bandwidth, we run the inversion for a maximum of 25 iterations using a nonlinear conjugate gradient algorithm. To mimic the measured wavefields, first, we computed observed data with free surface boundary conditions using

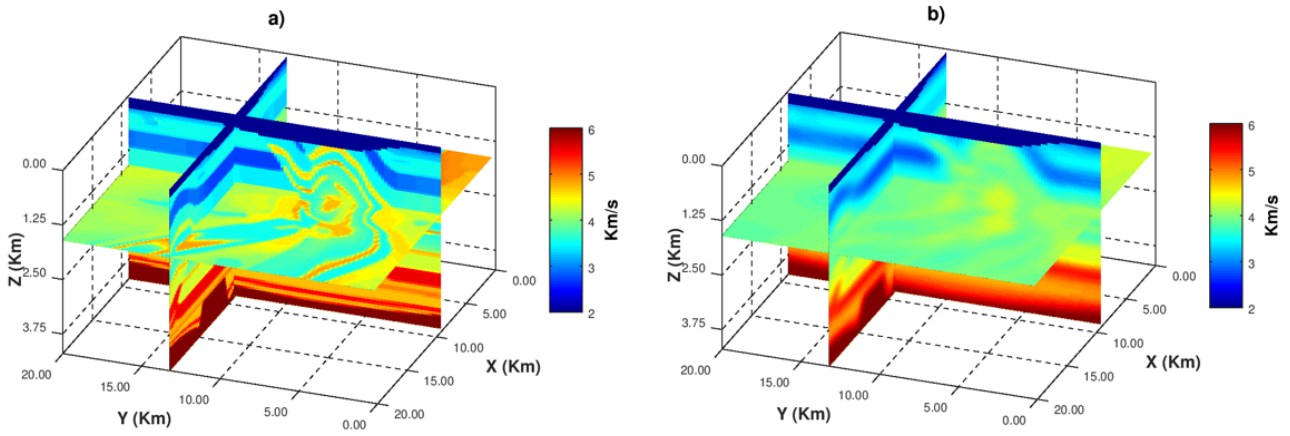

Figure 1: SEG/EAGE Overthrust velocity model with topography (blue in the top). True velocity model (a) and smooth velocity model used as the starting model for the inversion (b).

the exact source and receiver locations with the ghost interpolation scheme (see Figure 1a). Sources and receivers are not necessarily placed on the numerical Cartesian grid nodes.

Figure 2a is the reconstructed velocity model by FWI with ghost extrapolation method when source and receiver positions placed to their nearest grid nodes. Figure 2b is the reconstructed velocity model with the exact implementation of the source and receiver positions, and without the use of ghost extrapolation during modeling. Figure 2c is the reconstructed velocity model by FWI with the accurate implementation of arbitrary source and receiver locations at their exact positions and with the use of ghost wavefield value extrapolations near the free surface boundary. As we see in Figure 1c, the resolution of the retrieved model is substantially enhanced, and an accurate reconstructed velocity model is achieved with the use of irregular free surface treatment and with exact representations of source and receiver locations in the numerical forward modeling.

Conclusion

In this paper, we present a 3D acoustic time-domain FWI suitable for land exploration. For land FWI, the efficiency and accuracy of subsurface model reconstruction from FWI require the accuracy of numerical simulation of the seismic wavefield that takes into account for effects of complex surface topography. The standard finite-difference scheme computing seismic wave propagation in the earth implicitly assumes uniform structured grids and often provides diffraction artifacts generated by the staircase boundary. Accurate source and receiver location implementations are also crucial for the successful application of 3D FWI to land explorations. In this work, to avoid numerical artifacts generates from the finite-difference approximation near the irregular topographic surface, staircase boundary treatment is implemented to handle the irregular free boundary in the computation domain, which is discretized using a regular Cartesian grid. The ghost cell wavefield values beyond the free surface are interpolated using an accurate Lagrange interpolation method in three dimensions. In addition to the accurate implementation of arbitrary source and receiver locations at their exact positions, the use of ghost wavefield value extrapolations at and near the free surface boundary in the finite-difference approximation has shown a substantial improvement in terms of resolution and accuracy of the reconstructed velocity mode by FWI.

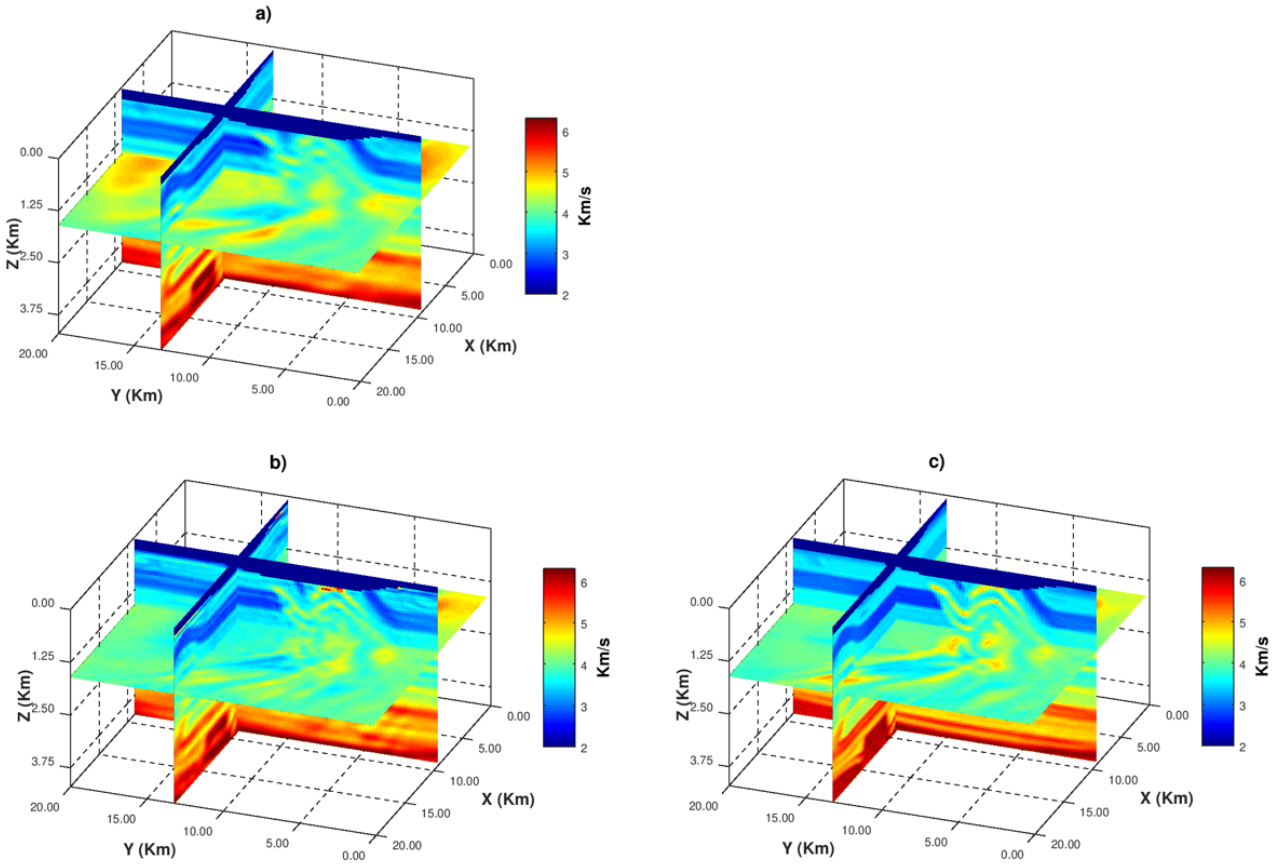

Figure 2: FWI results. (a) Reconstructed velocity model obtained by approximating source and receiver positions to its nearest grid nodes, and using the ghost extrapolation method. (b) Reconstructed velocity model using exact the source and receiver positions, and without ghost extrapolation method. (c) Reconstructed velocity model using exact source and receiver positions, and using the ghost extrapolation method.

Acknowledgements

The authors would like to thank Future Energy Systems research under the Canada First Research Excellence Fund (CFREF) for supporting this project.

References

Bergen, S. W. A., and A. Antoniou, 2005, Design of nonrecursive digital filters using the ultraspherical window function: EURASIP Journal on Advances in Signal Processing, **2005**, 1–13.

Bunks, C., F. M. Saleck, S. Zaleski, and G. Chavent, 1995, Multiscale seismic waveform inversion: Geophysics, **60**, 1457–1473.

Hicks, G. J., 2002, Arbitrary source and receiver positioning in finite-difference schemes using kaiser windowed sinc functions: GEOPHYSICS, **67**, 156–165.

Lemaistre, L., J. Brunellière, F. Studer, and C. Rivera, 2018, *in* FWI on land seismic datasets with topography variations: Do we still need to pick first arrivals?: 1078–1082.

Nocedal, J., and S. J. Wright, 2006, Numerical optimization, 2nd ed.: Springer.

Stekl, I., and R. G. Pratt, 1998, Accurate viscoelastic modeling by frequency-domain finite differences using rotated operators: Geophysics, **63**, 1779–1794.

Vigh, D., E. W. Starr, and J. Kapoor, 2009, Developing Earth models with full waveform inversion: The Leading Edge, **28**, 432–435.

Virieux, J., and S. Operto, 2009, An overview of full-waveform inversion in exploration geophysics: Geophysics, **74**, WCC1–WCC26.

Zhang, Q.-J., S.-K. Dai, L.-W. Chen, K. Li, D.-D. Zhao, and X.-X. Huang, 2015, Two-dimensional frequency-domain acoustic full-waveform inversion with rugged topography: Applied Geophysics, **12**, 378–388.